

Single-atom Catalysts with Hollow Rod/Plate like Structure for Enhanced Oxygen Reduction Reaction Performance in Zinc Air Battery

Muhammad Arif Khan^{1, a}, Guopu Cai^{1, b}, Rida Javed^d, Daixin Ye^{c, *}, and Hongbin Zhao^{b, *}, and Jiujun Zhang^c

a School of Materials Science and Engineering, Shanghai University, Shanghai 200444, PR China;

b Department of Chemistry, College of Sciences, Shanghai University, Shanghai 200444, PR China;

c College of Sciences & Institute for Sustainable Energy, Shanghai University, Shanghai 200444, PR China;

d College of Materials science and Engineering, Shenzhen university, Shenzhen, Guangdong, PR China;

Experimental

Synthesis of Co-N-C SAC

Cobalt hydroxide nanoplates $\text{Co}(\text{OH})_2$ were synthesized through hydrothermal method. In an experiment, 60 ml of DI water was taken in a beaker and 2.18 g of $\text{CoCl}_2 \cdot 6\text{H}_2\text{O}$ was dissolved in it through ultra-sonication for 3 minutes. After that 3 ml of the $\text{N}(\text{CH}_2\text{CH}_3)_3$ was added to the above solution and stirred for 2 h. It was then transferred to 100 ml Teflon vessel and hydrothermal treatment was done at 180°C for 24 h. The pink precipitate obtained after centrifugation with ethanol and DI water followed by drying at 80°C on oven is named as $\text{Co}(\text{OH})_2$ nanoplates.

In the second step, 300 mg of $\text{Co}(\text{OH})_2$ nanoplates and 15 mg of SDS were dispersed in 100 ml of DI water through stirring at room temperature for 4 h. Aniline monomer (90 μL), 1 ml H_2SO_4 solution (0.1 M), and 250 mg of APS were added to the above solution

and stirred for 2 h to complete the aniline polymerization. A black precipitate was obtained through centrifugation with DI water and ethanol followed by drying at 80°C. Co-N-C SAC was obtained after pyrolysis at 500°C for 2 h followed by acid leaching.

Synthesis of Ni-N-C SAC

Nickel hydroxide nanoplates $\text{Ni}(\text{OH})_2$ were synthesized through hydrothermal method. In an experiment, 60 ml of DI water was taken in a beaker and 1.98 g of $\text{NiCl}_2 \cdot 6\text{H}_2\text{O}$ was dissolved in it through ultra-sonication for 3 minutes. After that 3 ml of the $\text{N}(\text{CH}_2\text{CH}_3)_3$ was added to the above solution and stirred for 2 h. It was then transferred to 100 ml Teflon vessel and hydrothermal treatment was done at 170°C for 24 h. The green precipitate obtained after centrifugation with ethanol and DI water followed by drying at 80°C on oven is named as $\text{Ni}(\text{OH})_2$ nanoplates.

The Ni-N-C SAC formation process is same as explained for Co-N-C SAC.

Synthesis of Mn-N-C SAC

Hydrothermal method was used to synthesize Manganese oxide (MnO_2) nanorods. In an experiment, 1.69 g of $\text{MnSO}_4 \cdot \text{H}_2\text{O}$, 0.275 g of $(\text{NH}_4)_2\text{S}_2\text{O}_8$, and 0.315 g of $(\text{NH}_4)_2\text{S}_2\text{O}_8$ were added in 60 ml of DI water and stirred for 3 h. This solution was hydrothermally treated at 160°C for 16 h. The black precipitate obtained after centrifugation with ethanol and DI water followed by drying at 80°C is named as MnO_2 nanorods.

The synthesis process for Mn-N-C SAC is same as described for Co-N-C SAC.

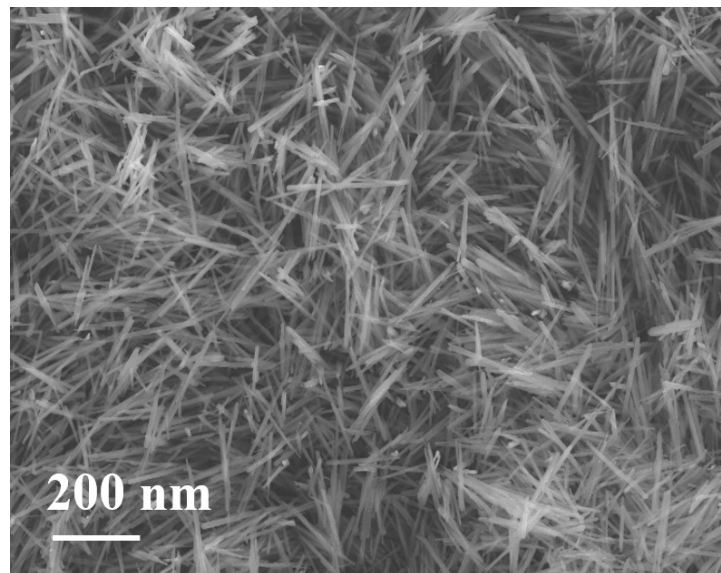


Fig. S1. SEM image for FeOOH.

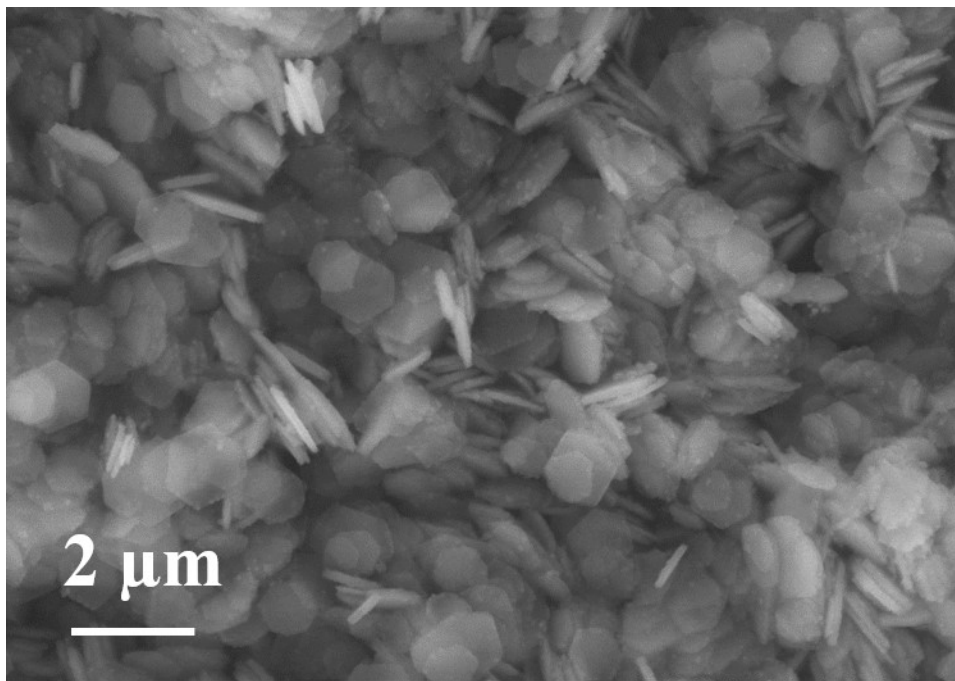


Fig. S2. SEM of Co(OH)_2 .

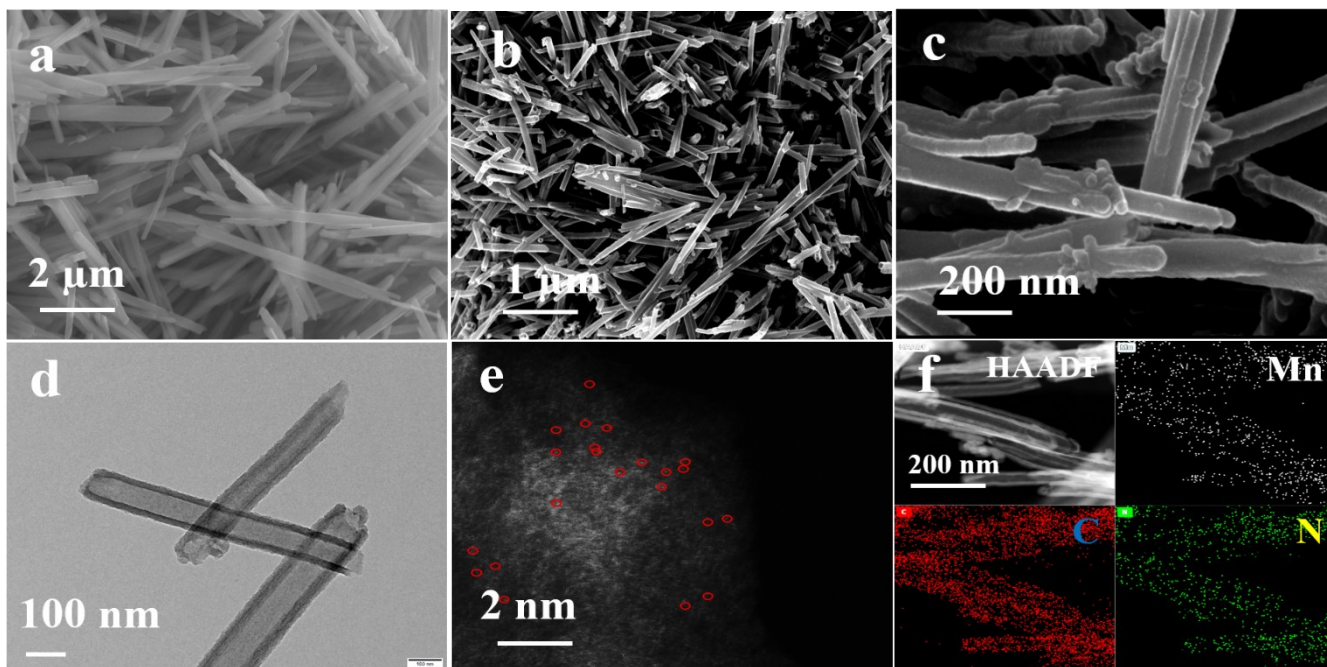


Fig. S3. (a) SEM of MnO₂; (b,c) SEM of Mn-N-C SAC; (d) TEM of Mn-N-C SAC; (e) Aberration corrected HAADF-STEM image of Mn-N-C SAC; (f) HAADF-STEM image and corresponding EDX mapping of Mn-N-C SAC.

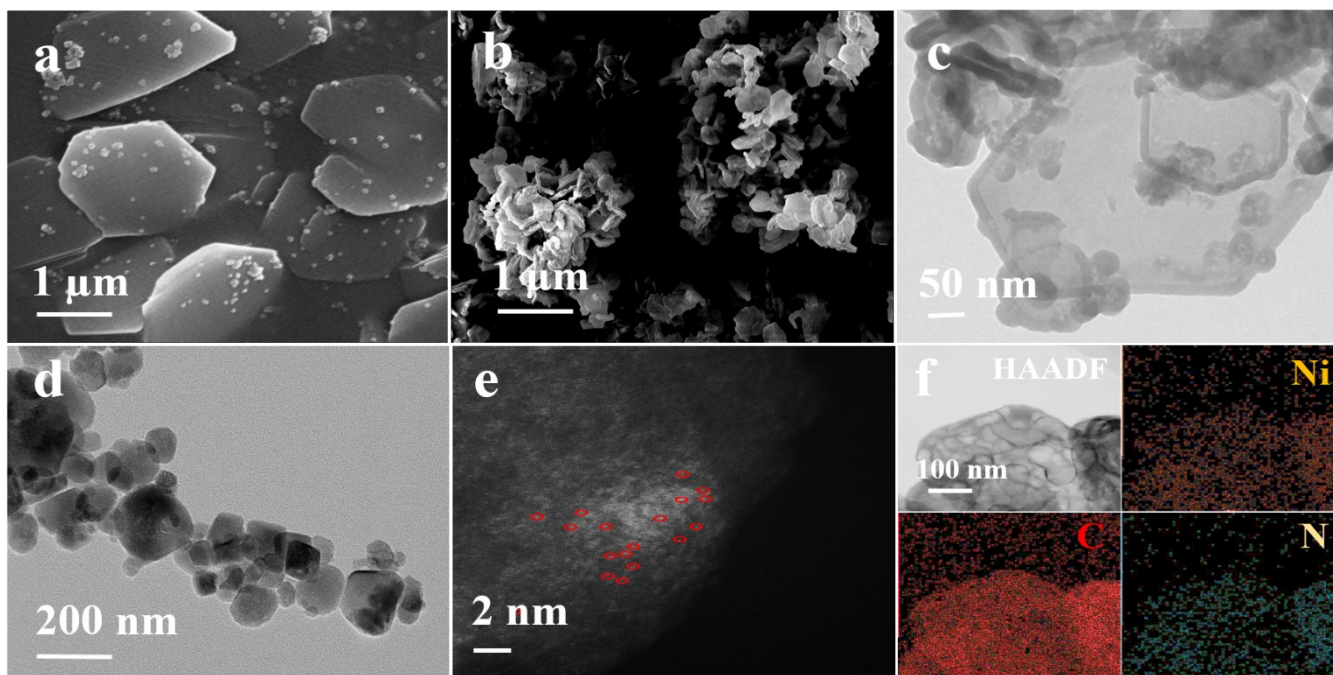


Fig. S4. (a) SEM of Ni(OH)₂; (b) SEM of Ni-N-C SAC; (c, d) TEM of Ni-N-C SAC; (e) Aberration corrected HAADF-STEM image of Ni-N-C SAC; (f) HAADF-STEM image and corresponding EDX mapping of Ni-N-C SAC.

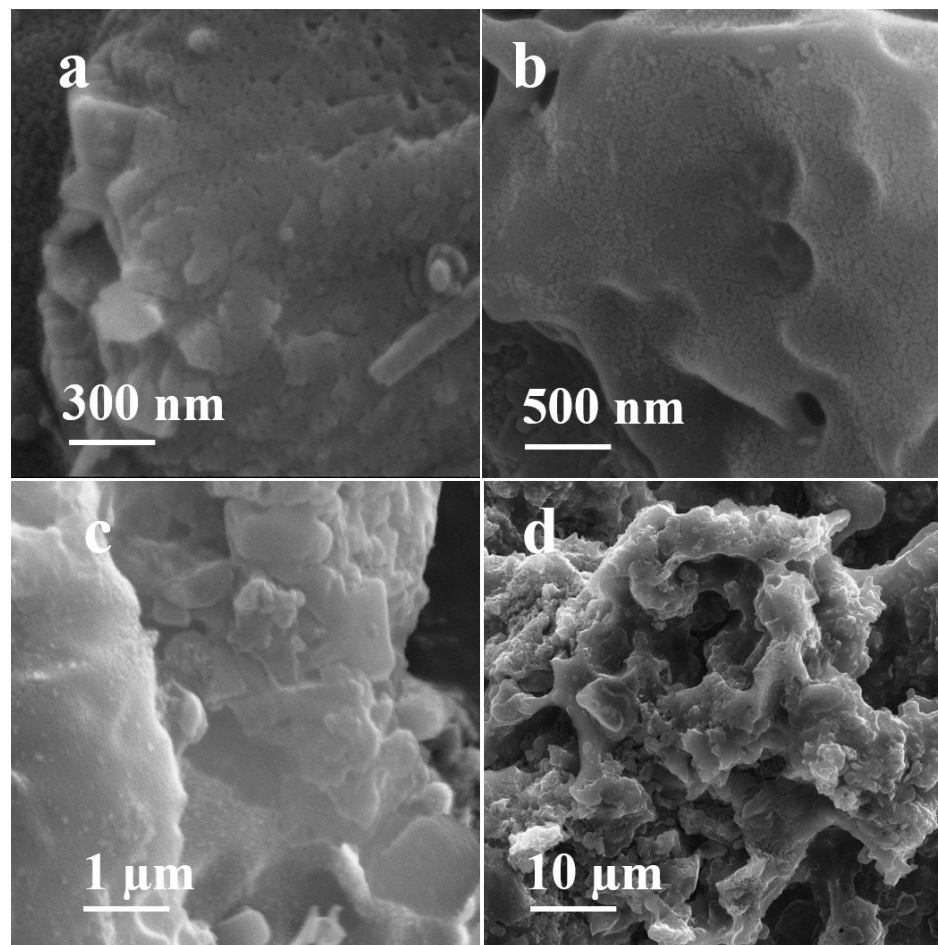


Fig. S5. SEM of NC sample.

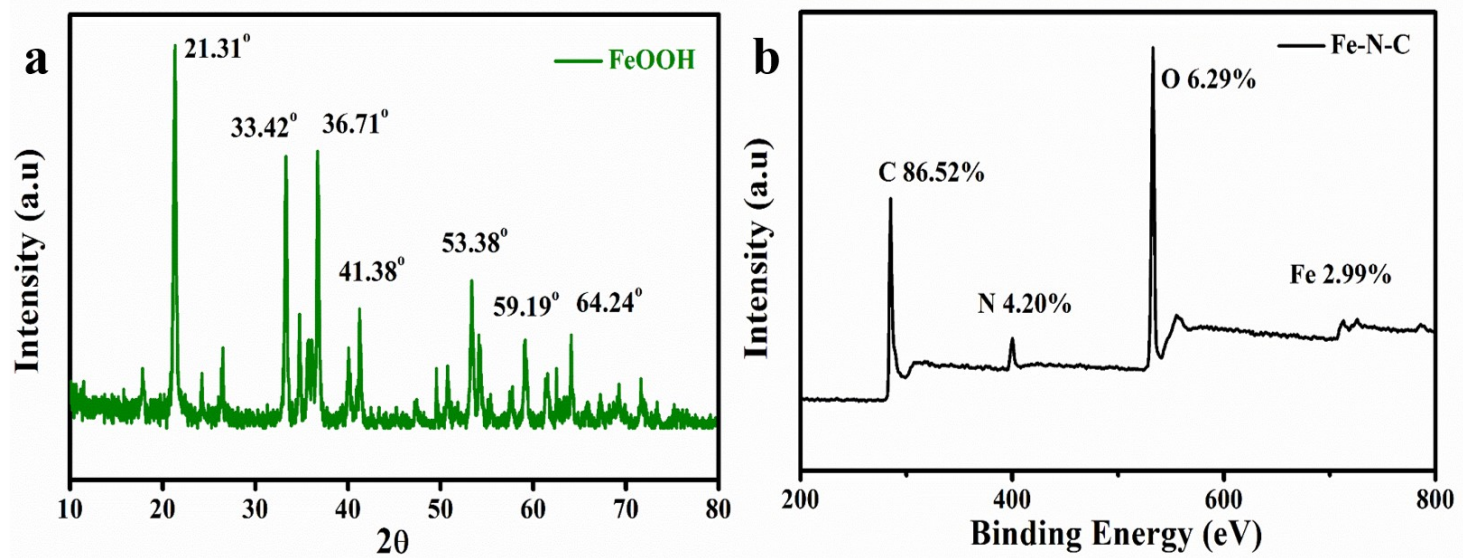


Fig. S6. (a) XRD of FeOOH; (b) XPS survey of Fe-N-C SAC.

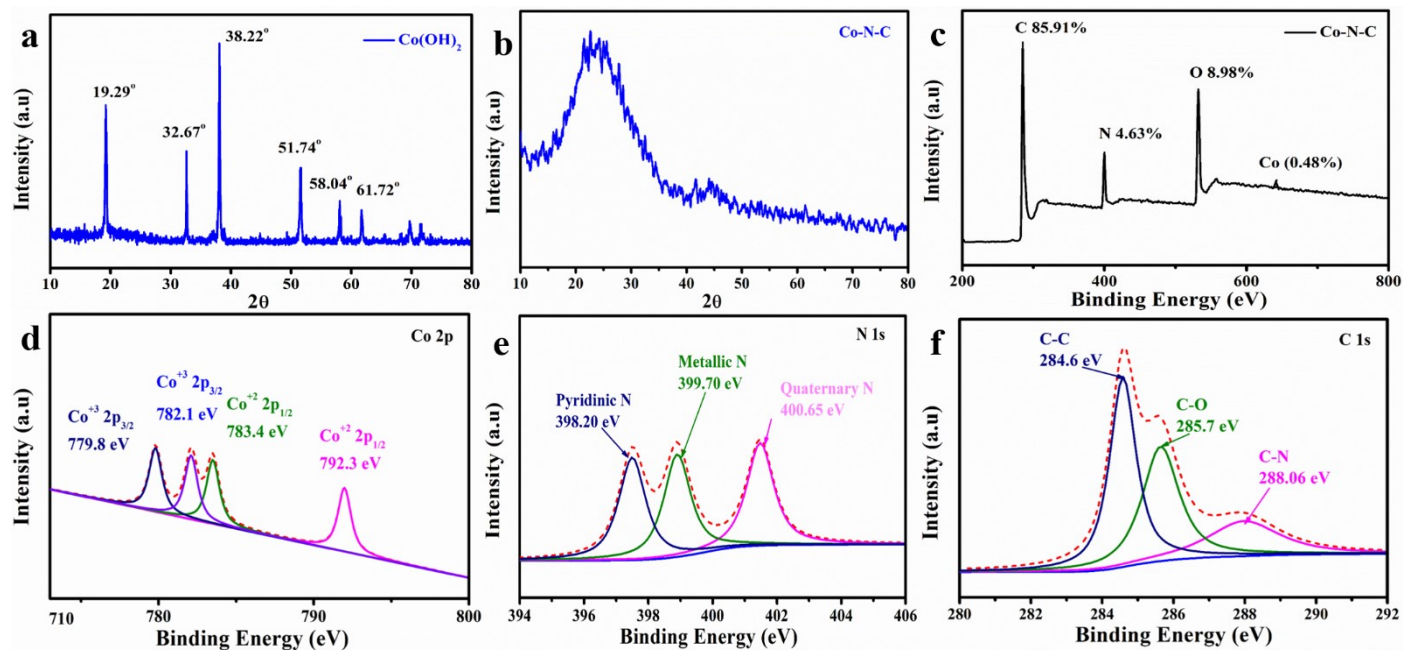


Fig. S7. XRD pattern of (a) Co(OH)_2 ; (b) Co-N-C SAC; (c) XPS survey of Co-N-C SAC; (d-f) Co 2p, N 1s, and C 1s of Co-N-C SAC.

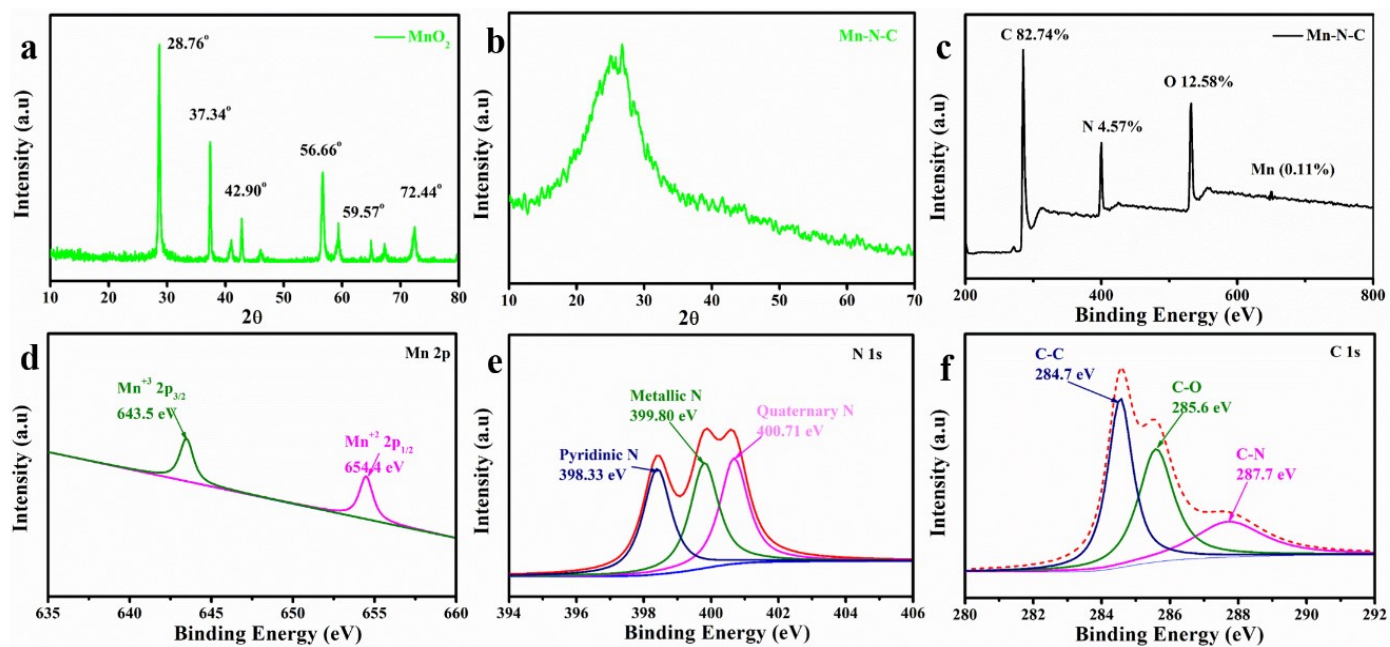


Fig. S8. XRD pattern of (a) MnO₂; (b) Mn-N-C SAC; (c) XPS survey of Mn-N-C SAC; (d-f) Mn 2p, N 1s, and C 1s of Mn-N-C SAC.

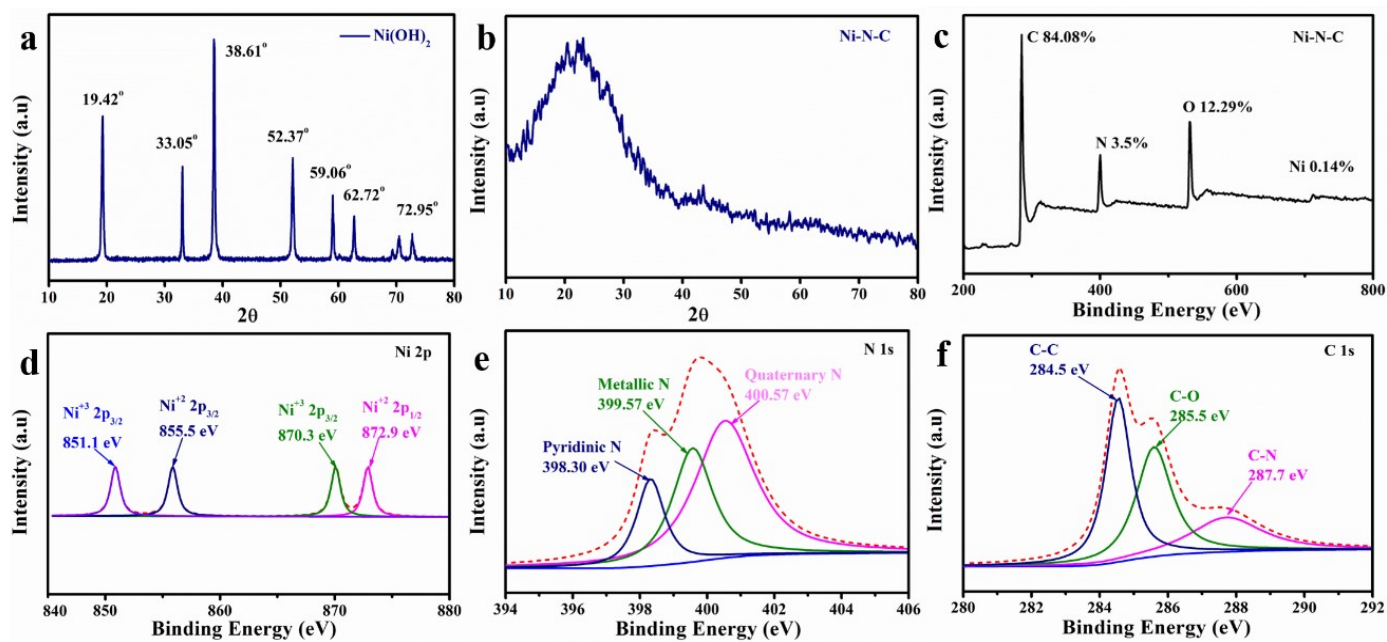


Fig. S9. XRD pattern of (a) Ni(OH)_2 ; (b) Ni-N-C SAC; (c) XPS survey of Ni-N-C SAC; (d-f) Ni 2p, N 1s, and C 1s of Ni-N-C SAC.

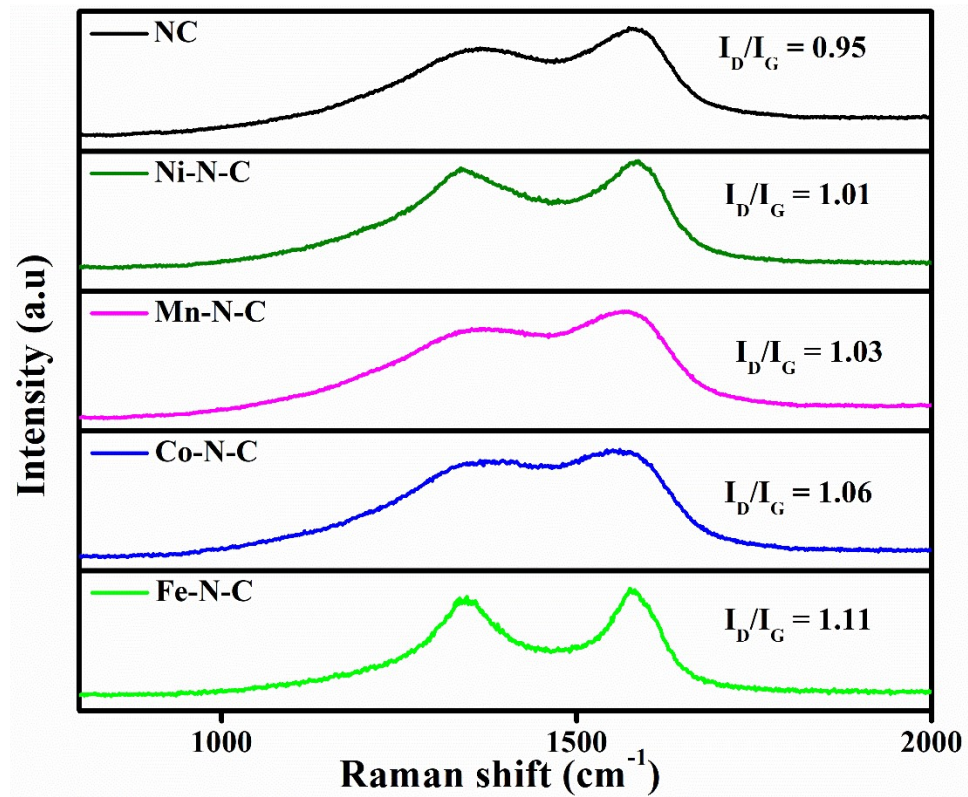


Fig. S10. Raman analysis results for Fe-N-C, Co-N-C, Mn-N-C, Ni-N-C, and NC.

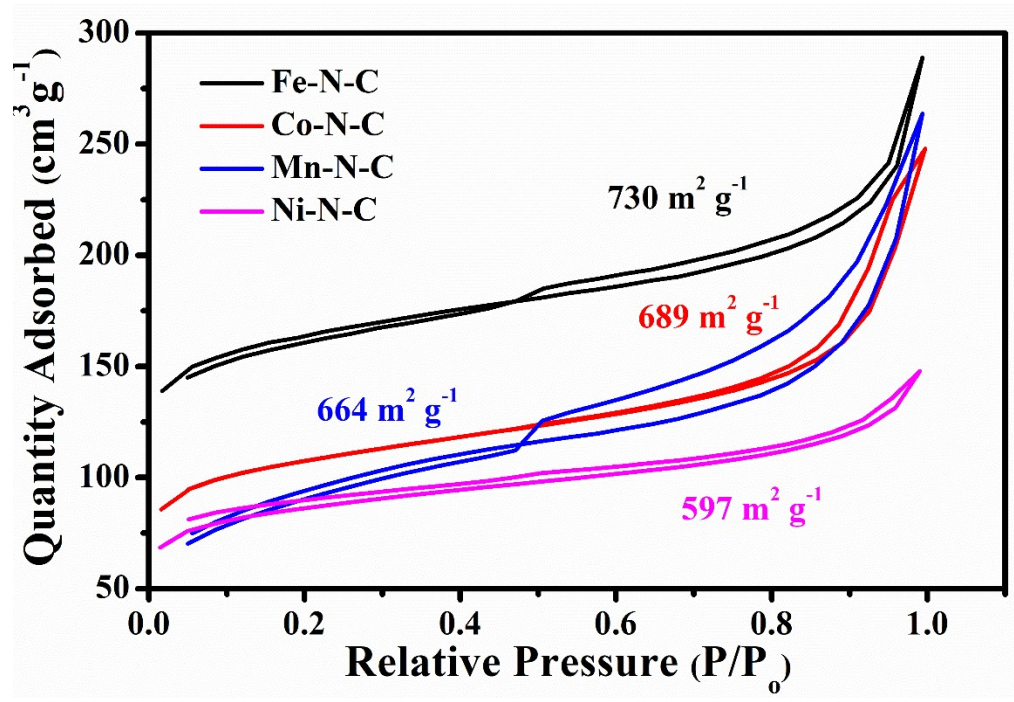


Fig. S11. N₂ adsorption-desorption isotherms for Fe-N-C SAC, Co-N-C SAC, Mn-N-C SAC, and Ni-N-C SAC.

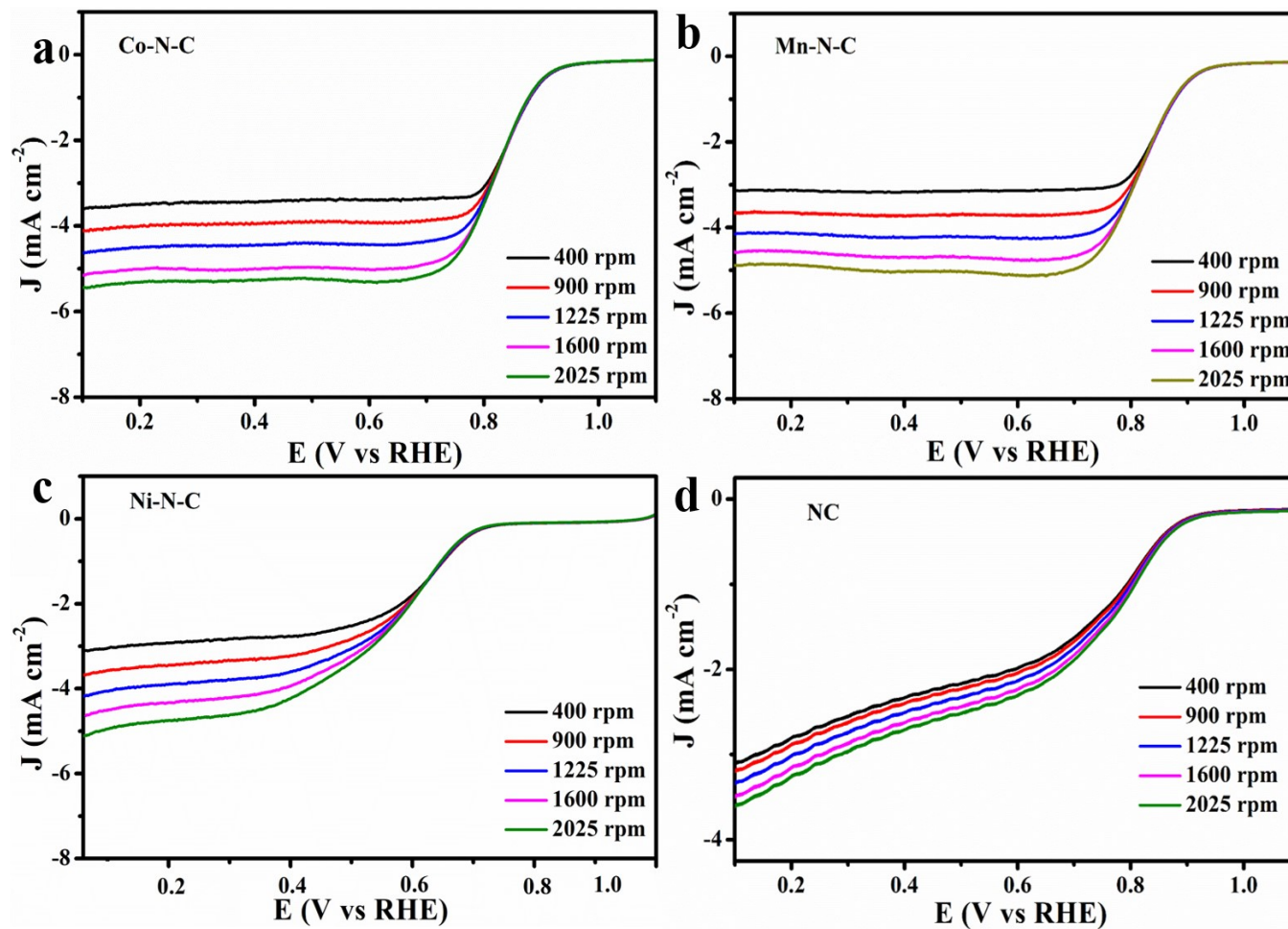


Fig. S12. LSV curves at different rpm in O₂ saturated 0.1 M KOH solution for (a) Co-N-C SAC; (b) Mn-N-C SAC; (c) Ni-N-C SAC; (d) NC.

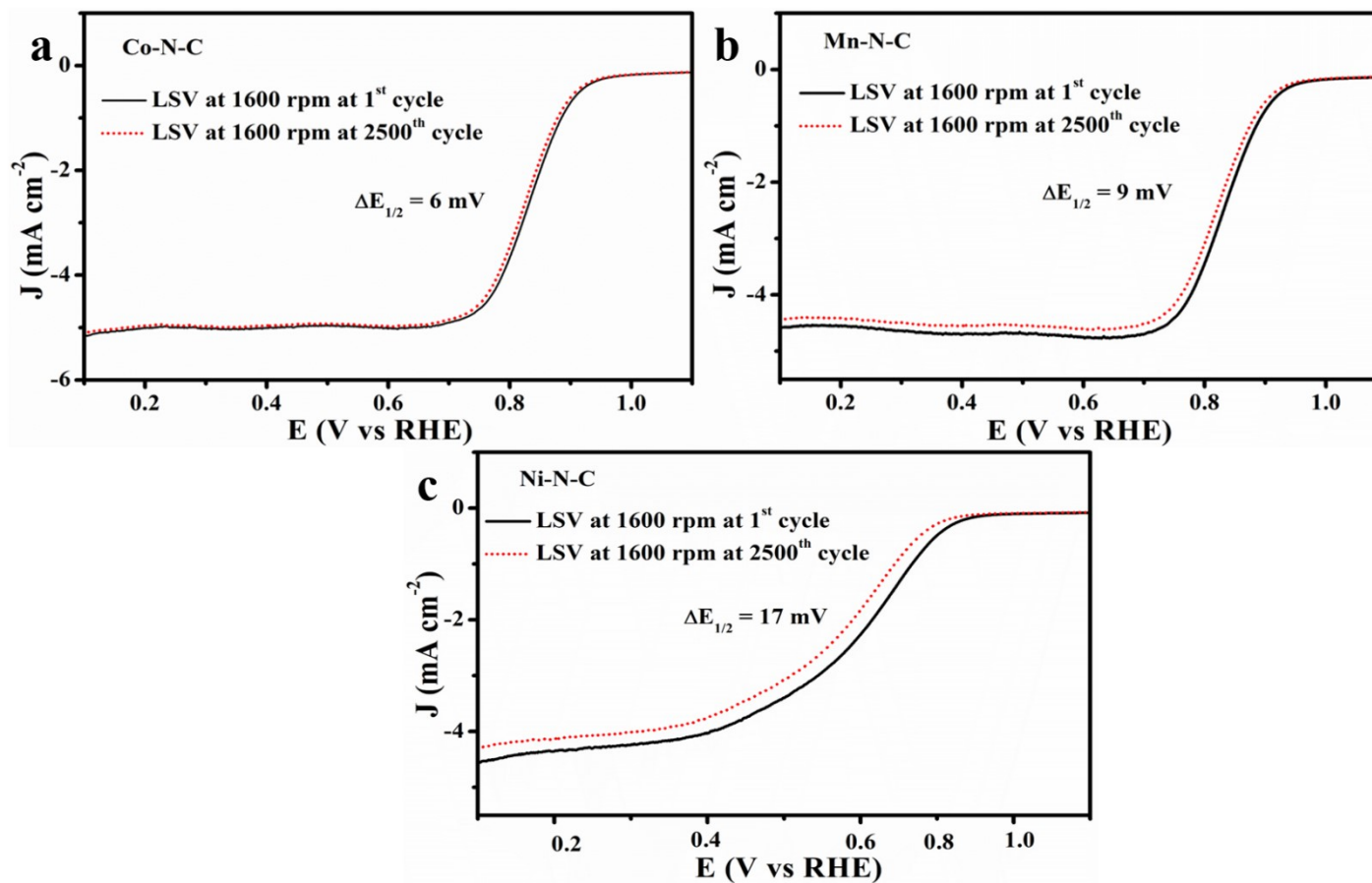


Fig. S13. LSV curves at 1600 rpm at 1st cycle and at 2500th cycle in O₂ saturated 0.1 M KOH solution for (a) Co-N-C SAC; (b) Mn-N-C SAC; (c) Ni-N-C SAC.

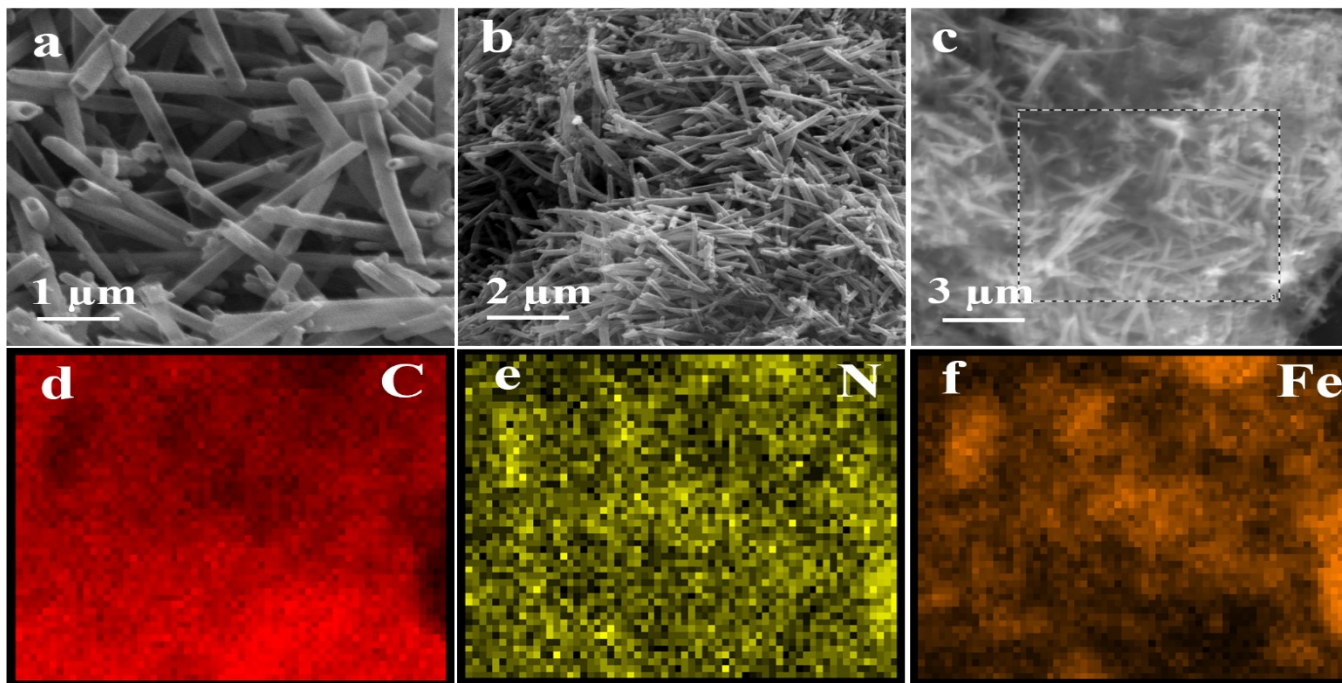


Fig. S14. (a, b) SEM for Fe-N-C after stability test of 2500th cycle, (c-f) corresponding EDS mapping.

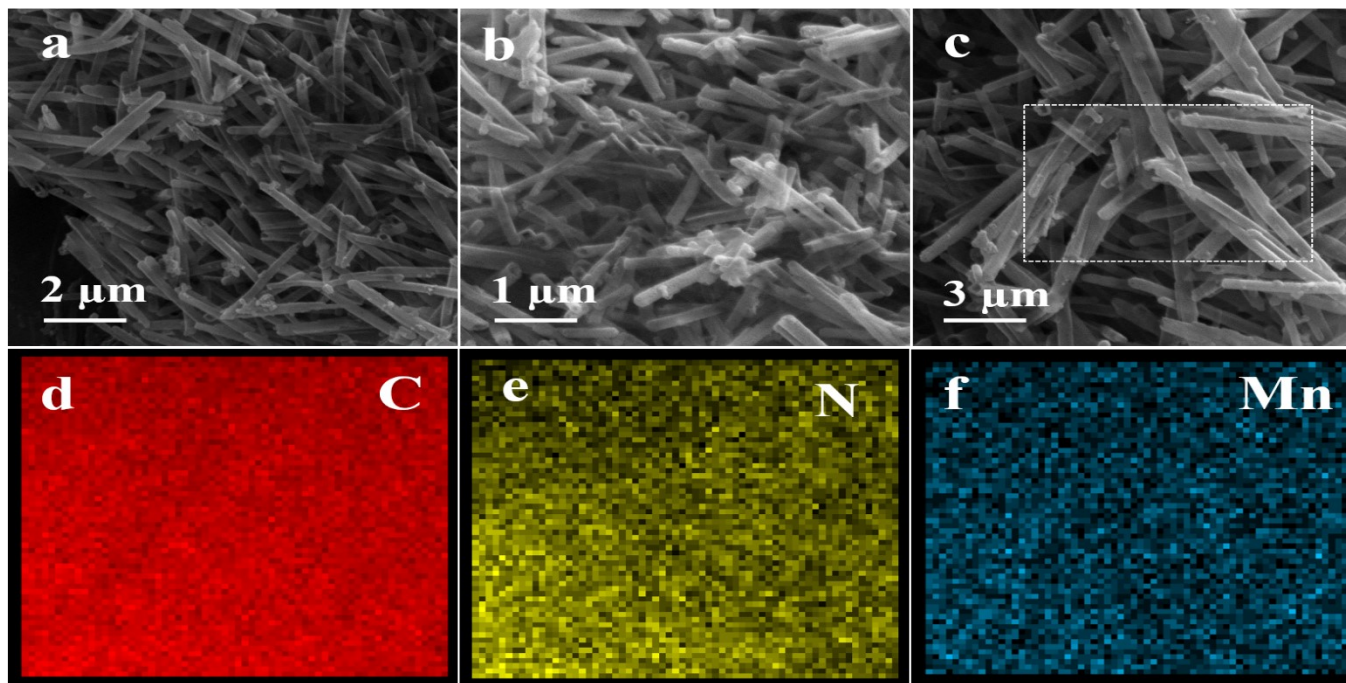


Fig. S15. (a, b) SEM for Mn-N-C after stability test of 2500th cycle, (c-f) corresponding EDS mapping.

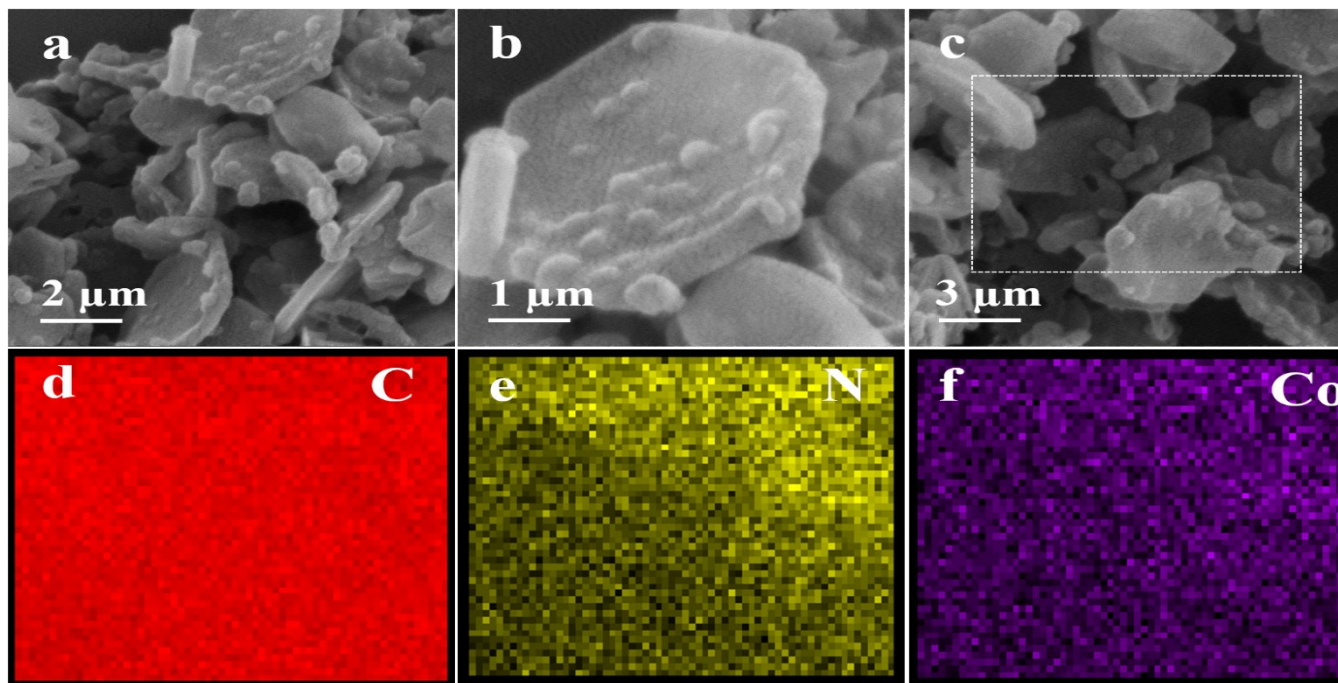


Fig. S16. (a, b) SEM for Co-N-C after stability test of 2500th cycle, (c-f) corresponding EDS mapping.

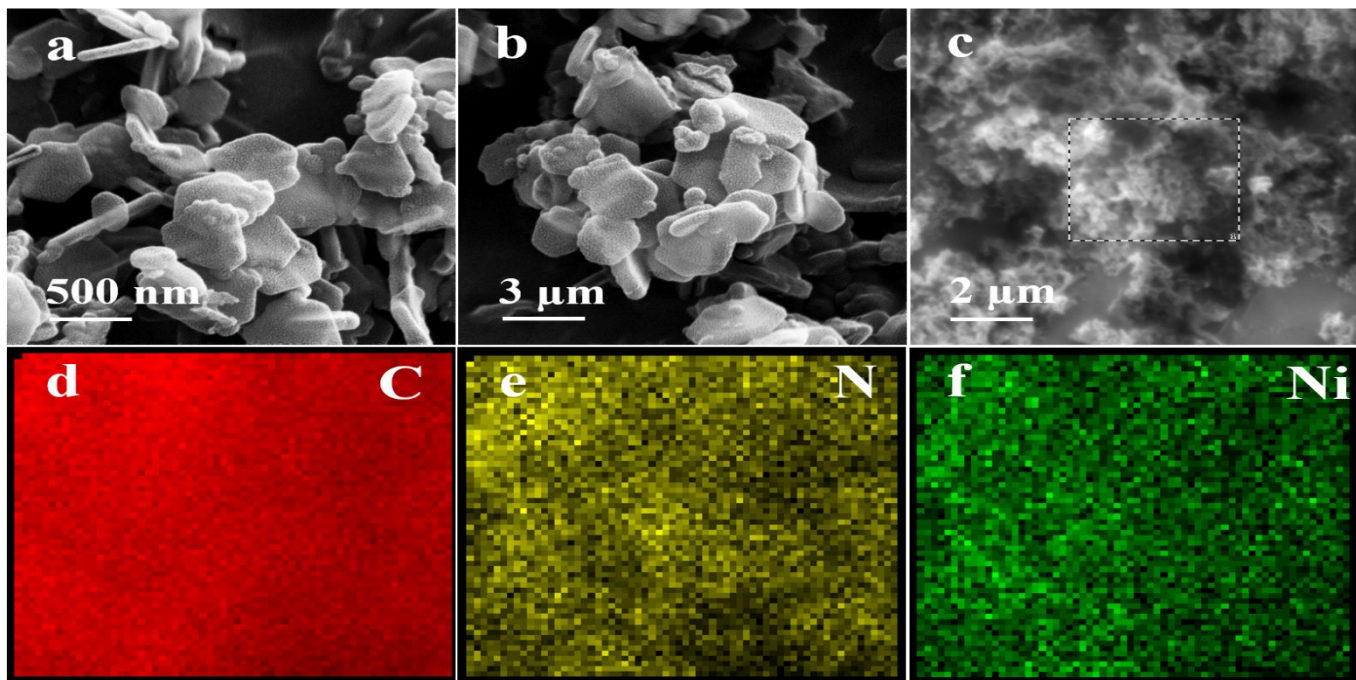


Fig. S17. (a, b) SEM for Ni-N-C after stability test of 2500th cycle, (c-f) corresponding EDS mapping.

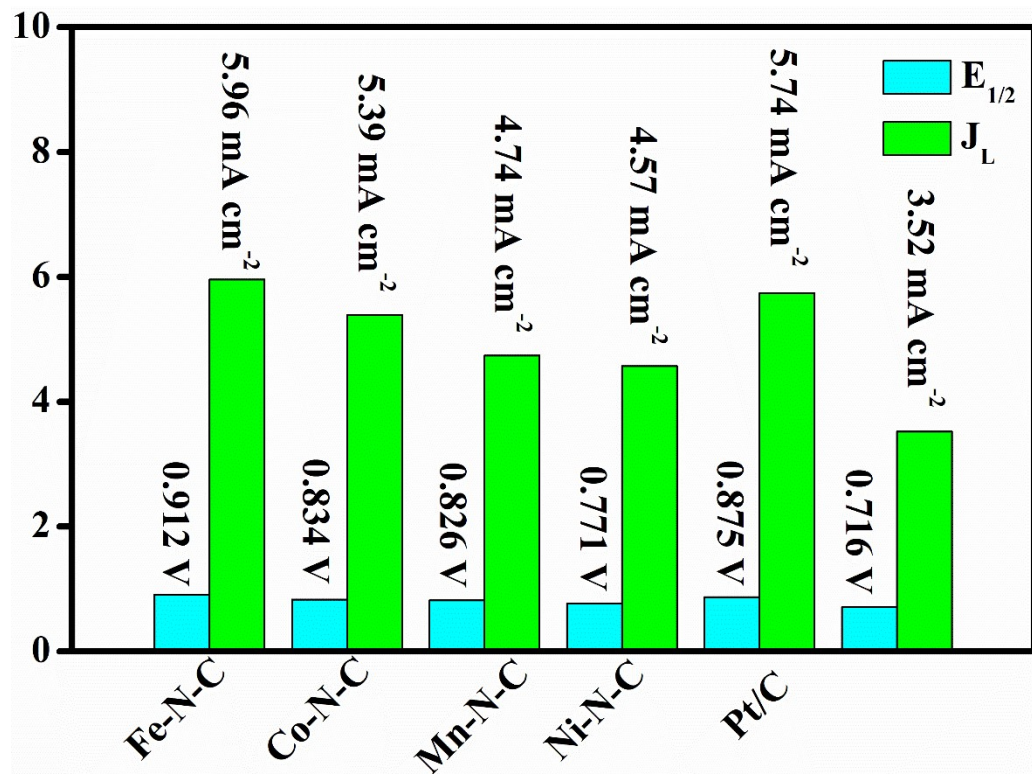


Fig. S18. Comparative ORR catalytic performance in O_2 saturated 0.1 M KOH solution for the Fe-N-C SAC, Co-N-C SAC, Mn-N-C SAC, Ni-N-C SAC, 20% Pt/C, and NC.

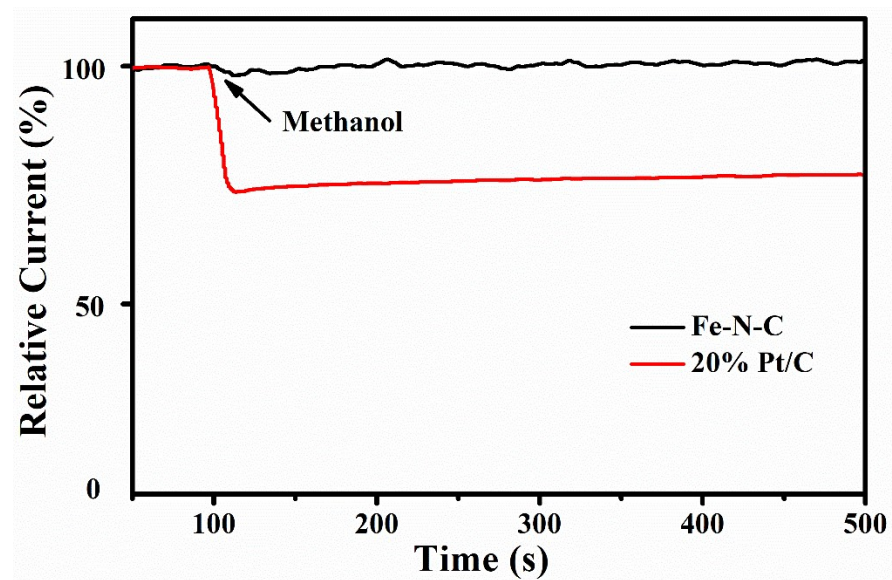


Fig. S19. Methanol tolerance test for Fe-N-C SAC and 20% Pt/C.

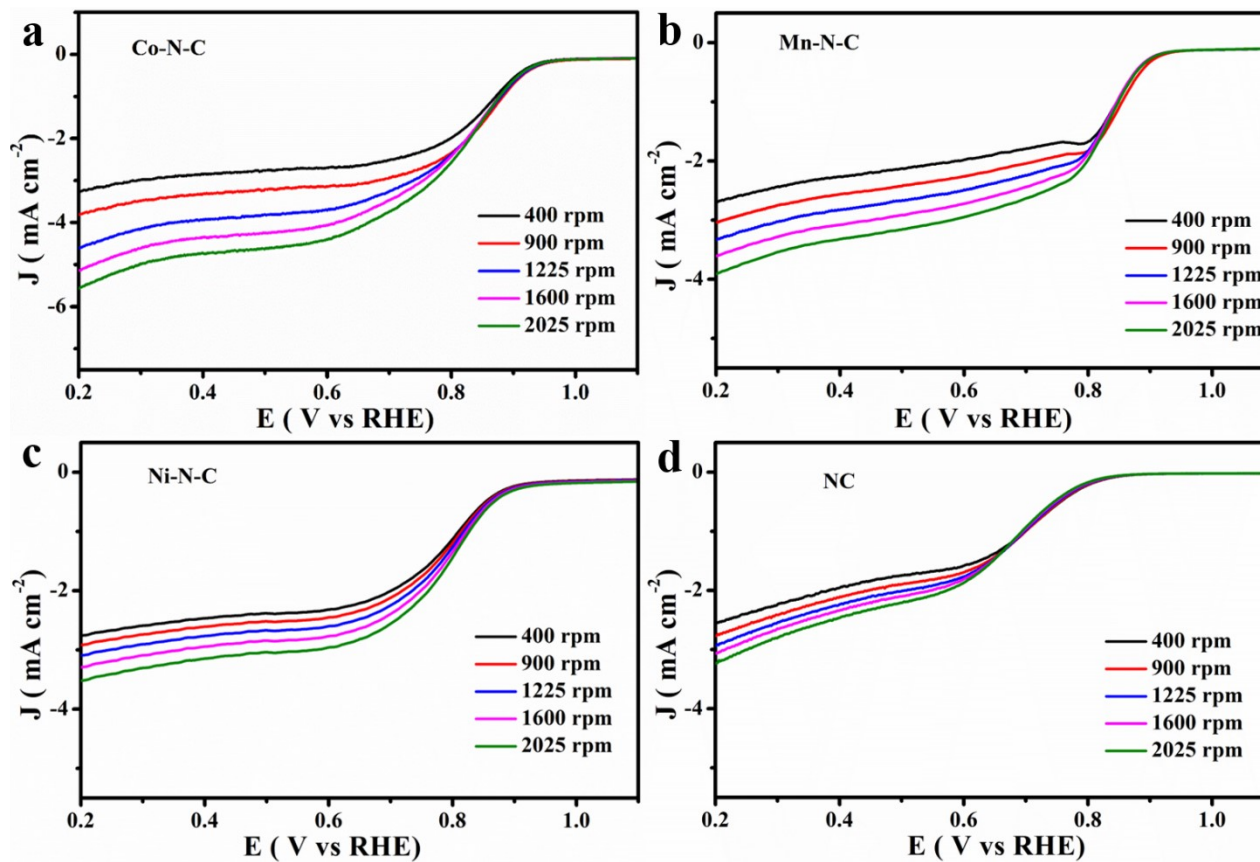


Fig. S20. LSV curves at different rpm in O_2 saturated 0.1 M HClO_4 solution for (a) Co-N-C SAC; (b) Mn-N-C SAC; (c) Ni-N-C SAC; (d) NC.

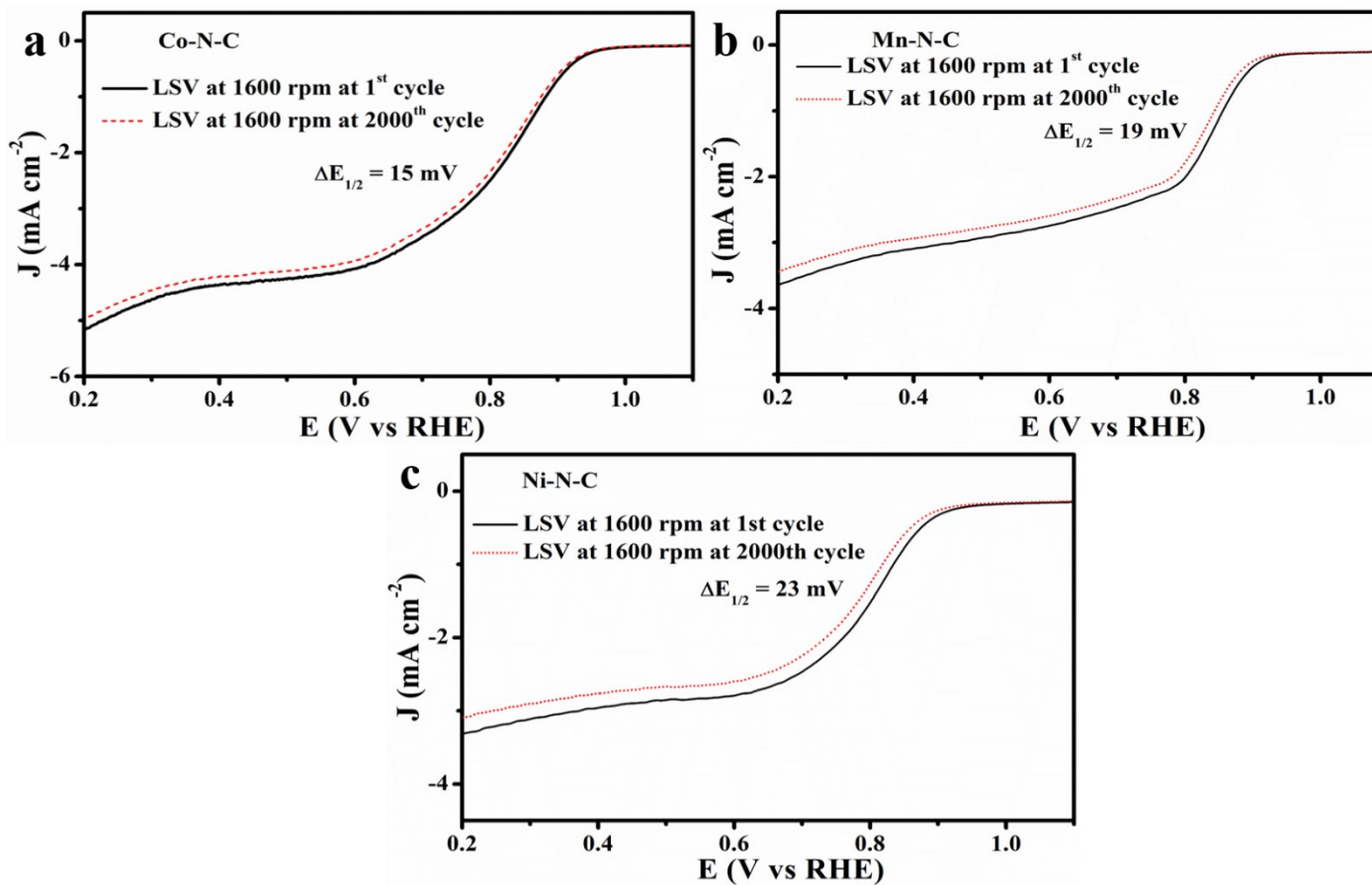


Fig. S21. LSV curves at 1600 rpm at 1st cycle and after 2000th cycle in O₂ saturated 0.1 M HClO₄ solution for (a) Co-N-C SAC; (b) Mn-N-C SAC; (c) Ni-N-C SAC.

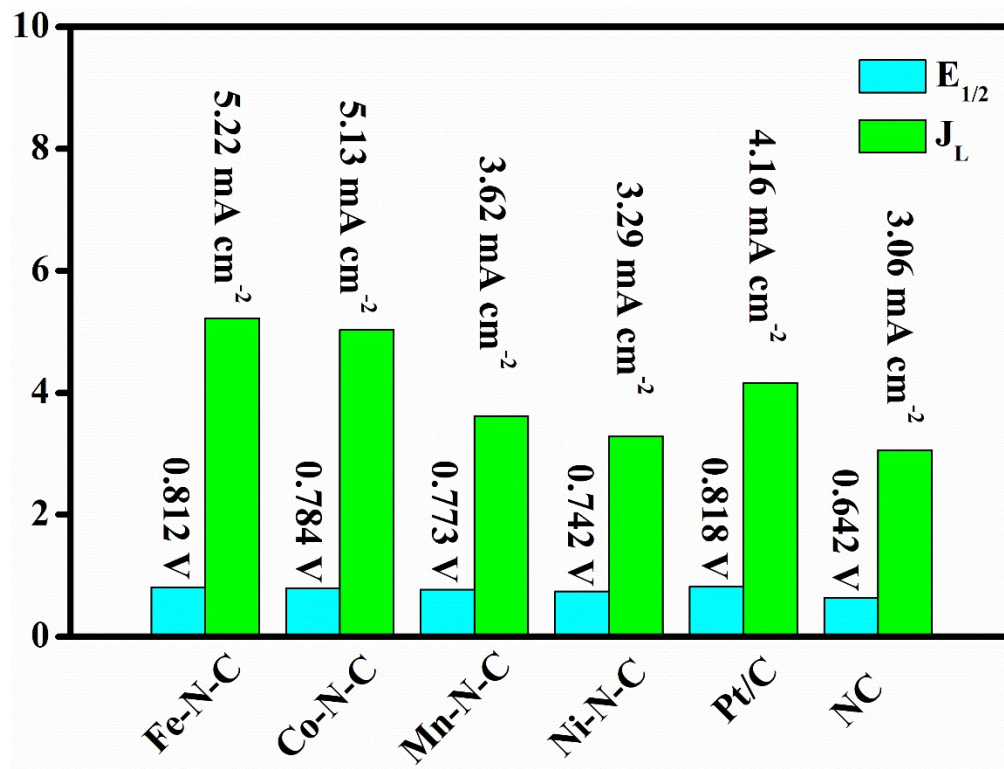


Fig. S22. Comparative ORR catalytic performance in O_2 saturated 0.1 M HClO_4 solution for Fe-N-C SAC, Co-N-C SAC, Mn-N-C SAC, Ni-N-C SAC, 20% Pt/C, and NC.

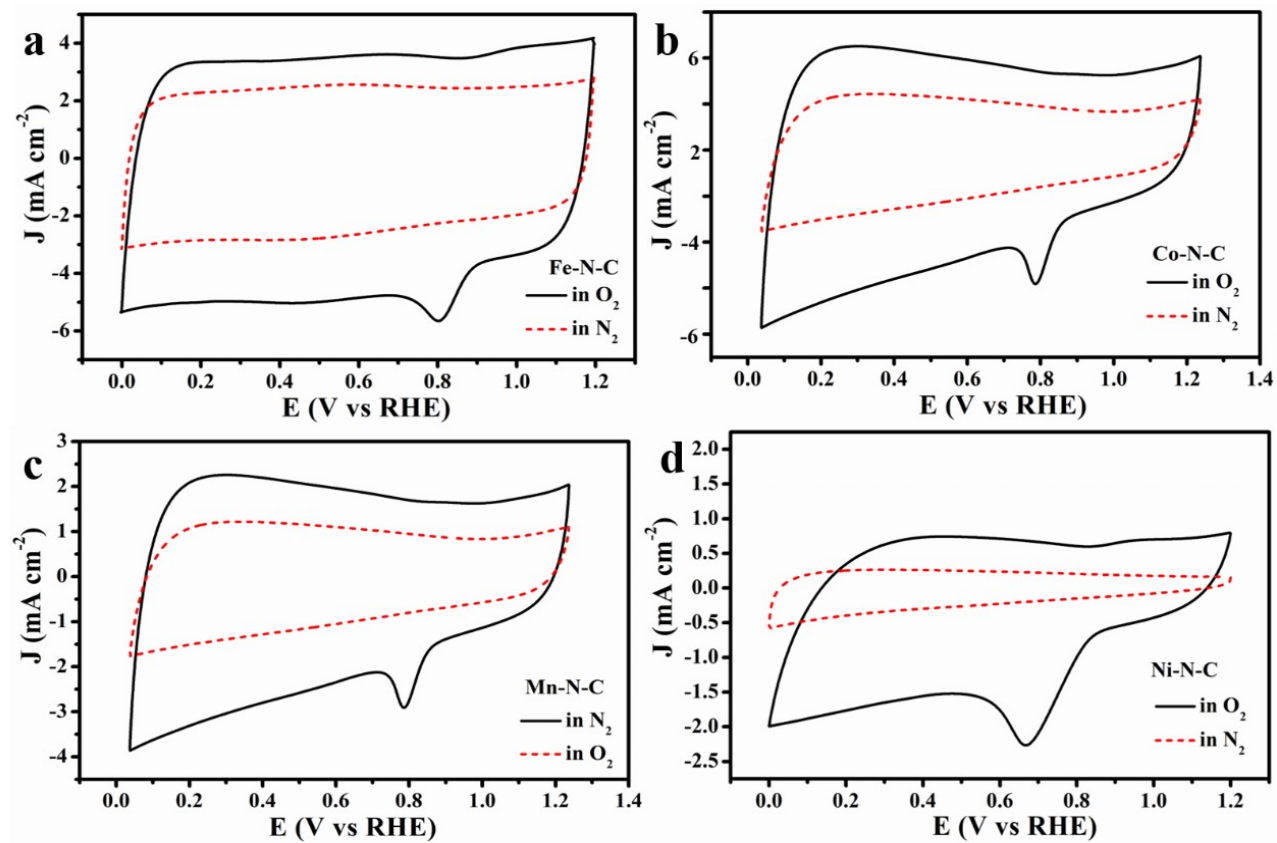


Fig. S23. CV curves in 0.1 M KOH for (a) Fe-N-C SAC; (b) Co-N-C SAC; (c) Mn-N-C SAC; (d) Ni-N-C SAC.

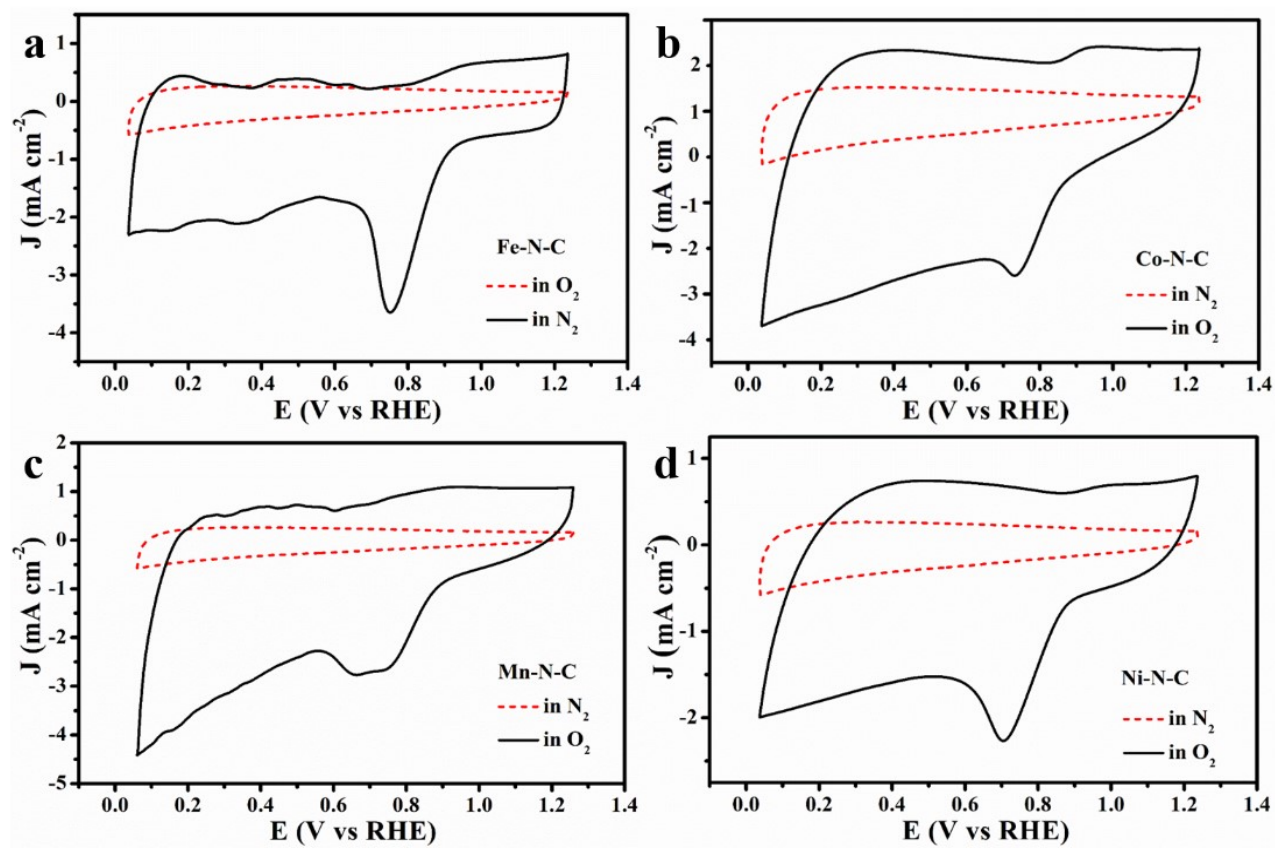


Fig. S24. CV curves in 0.1 M HClO_4 for (a) Fe-N-C SAC; (b) Co-N-C SAC; (c) Mn-N-C SAC; (d) Ni-N-C SAC.

Table S1: Fe atomic percentage from ICP-OES

Catalyst	Metal content (wt. %)
Fe-N-C	2.83
Co-N-C	0.97
Mn-N-C	0.86
Ni-N-C	0.79

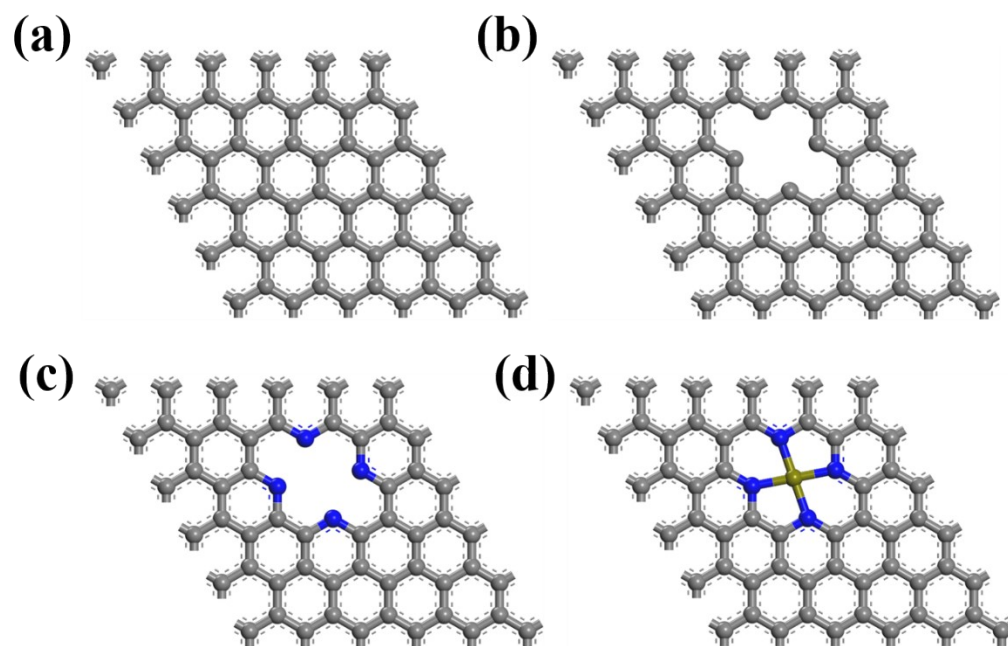


Fig. S25. (a) Graphene, (b) graphene quadruple vacancy (QV), (c) graphene quadruple vacancy (QV) with N atoms, (d) M-N-C. Grey: C, blue: N, and green: M (M = Fe, Co, Mn, and Ni) atoms, respectively.

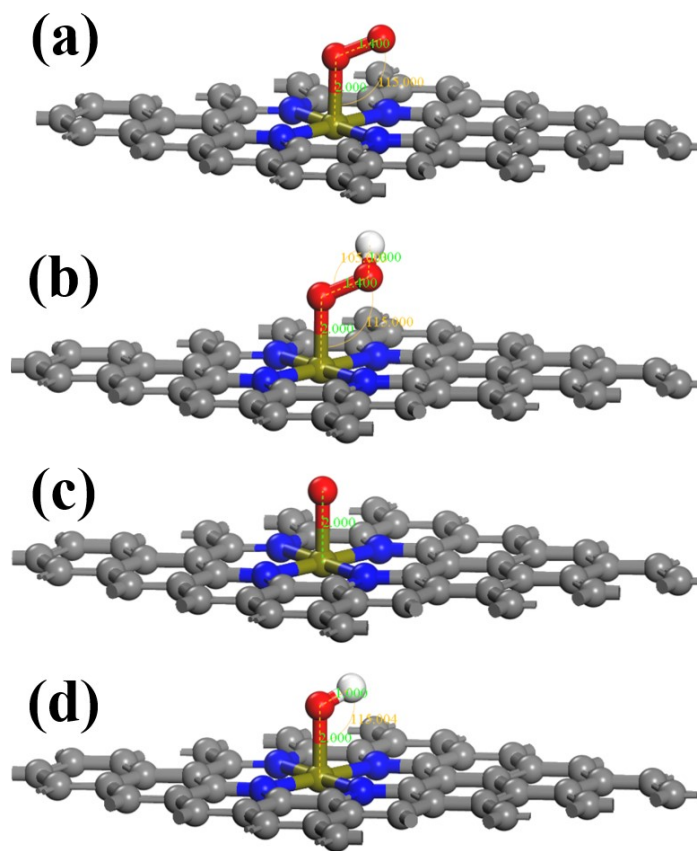


Fig. S26. Intermediates (a) O_2 , (b) $-OOH$, (c) O^* , and (d) OH^* on M-N-C.

Table S2: Comparative literature for M-N-C SAC catalyst

Catalyst	Loading amount of the catalyst (mg cm ⁻²)	E _{1/2} in acid (V)	E _{1/2} in base (V)	ZAB Performance (mW cm ⁻²)	Reference
Co@NC-MOF	0.6	0.72	0.88	-	1
Co-N-C	0.8	-	0.85	227	2
Co-N-C			0.82	135	3
Fe-N-C	0.6	0.80	0.88	-	4
Fe-N-C	0.65	-	0.82	-	5
Fe-N-C-NH ₃	0.4	0.65	0.85	-	6
Fe-N-C	0.4	-	0.87	185	7
Mn-N-C	0.6	-	0.81	-	8
Fe-N-C	0.6	-	0.83	71.6	9
Fe-N-C	0.5	-	0.89	-	10
Mn-N-C	0.8	0.74	-		11
Fe-N-C	0.4	0.80	0.91	185	This work

Co-N-C	0.78	0.83
Mn-N-C	0.77	0.82
Ni-N-C	0.72	0.76

References

1. S. G. Peera, J. Balamurugan, N. H. Kim and J. H. Lee, *Small*, 2018, **14**, e1800441.
2. C. Lei, R. Yang, J. Zhao, W. Tang, F. Miao, Q. Huang and Y. Wu, *Frontiers in Energy*, 2024, DOI: 10.1007/s11708-024-0928-6.
3. H. Wang, X. Zhang, X. Li, Y. Li, D. Kong, Z. Zhen, L. Geng, L. Zhi and Z. Li, *Renewables*, 2023, **1**, 353-361.
4. J.-W. Huang, Q.-Q. Cheng, Y.-C. Huang, H.-C. Yao, H.-B. Zhu and H. Yang, *ACS Applied Energy Materials*, 2019, **2**, 3194-3203.
5. C. Maouche, Y. Zhou, B. Li, C. Cheng, Z. Wu, X. Han, S. Rao, Y. Li, N. Rahman and J. Yang, *Journal of The Electrochemical Society*, 2022, **169**, 062501.
6. Z. Chen, D. Zhao, C. Chen, Y. Xu, C. Sun, K. Zhao, M. Arif Khan, D. Ye, H. Zhao, J. Fang, X. Andy Sun and J. Zhang, *Journal of colloid and interface science*, 2021, **582**, 1033-1040.
7. M. Arif Khan, C. Sun, J. Cai, D. Ye, K. Zhao, G. Zhang, S. Shi, L. Ali Shah, J. Fang, C. Yang, H. Zhao, S. Mu and J. Zhang, *ChemElectroChem*, 2021, **8**, 1298-1306.
8. L. Xiao, J.-M. Yang, G.-Y. Huang, Y. Zhao and H.-B. Zhu, *Inorganic Chemistry Communications*, 2020, **118**, 107982.
9. J. Li, M. Lin, W. Huang, X. Liao, Y. Ma, L. Zhou, L. Mai and J. Lu, *Small methods*, 2023, **7**, e2201664.

10. H. Gharibi, K. Tadavani, H. Balali Dehkordi and M. Zhiani, *Energy & Fuels*, 2023, **37**.
11. T. Stracensky, L. Jiao, Q. Sun, E. Liu, F. Yang, S. Zhong, D. A. Cullen, D. J. Myers, A. J. Kropf, Q. Jia, S. Mukerjee and H. Xu, *ACS Catalysis*, 2023, **13**, 14782-14791.